



# Epistemic uncertainty of Finite Element models to predict the seismic response of RC free-plan buildings

M. F. Chacón<sup>(1,a)</sup>, J. C. de la Llera<sup>(1,b)</sup>, and M. H. Hube<sup>(1,c)</sup>

<sup>(1)</sup> Department of Structural and Geotechnical Engineering, Pontificia Universidad Católica de Chile, and National Research Center for Integrated Natural Disaster Management CONICYT/FONDAP/15110017, Vicuña Mackenna 4860, Santiago, Chile.

<sup>(a)</sup> [mfchacon@uc.cl](mailto:mfchacon@uc.cl); <sup>(b)</sup> [jcllera@ing.puc.cl](mailto:jcllera@ing.puc.cl); <sup>(c)</sup> [mhube@ing.puc.cl](mailto:mhube@ing.puc.cl)

## Abstract

This study quantifies the epistemic uncertainty of several modeling assumptions in evaluating the seismic response of six reinforced concrete free-plan office buildings located in Santiago, Chile. The assumptions analyzed are: **(1)** the in-plane and out-of-plane stiffness of the diaphragms; **(2)** the simplified soil-structure interaction model; and **(3)** the level of fixity of the structure. Several detailed finite elements models were elaborated using the ETABS and ANSYS software packages and the seismic response was estimated using response spectrum analysis. The response uncertainty was evaluated by comparing predicted global and local seismic response parameters, such as story shears and drifts, between a predefined *reference* model commonly used in design with a set of *variant* models. A statistical evaluation of the modeling uncertainty showed a strong dependency on the response parameter considered, ranged from 11% to 112%. It was concluded also that uncertainties identified in the shear forces of walls at the elevator core were larger than uncertainties in total story shear forces. Additionally, larger uncertainty was identified for shear forces at the basements than shear at upper stories. The out-of-plane diaphragm stiffness was found as one of the most important sources of epistemic uncertainty for the core wall shear and total story shear in upper stories. Finally, the most significant source of uncertainty for the base shear is the one associated with the type of soil-structure interaction model used.

*Keywords:* epistemic uncertainty; free-plan buildings; diaphragm stiffness; soil-structure interaction; basement effect.

## 1. Introduction

Reinforced concrete (RC) free-plan buildings consist of shear walls as part of a building core, a RC moment-resisting perimeter frame, and a post tensioned floor slab that connect the core and perimeter frame (Figure 1 and 2c). Typical story heights range between 18 and 25 stories, and 4 to 8 stories, above and below ground, respectively. Fundamental vibration periods usually exceed 1.5s. Before to the  $M_w=8.8$  Maule earthquake (Chile, 2010), little information about the seismic performance of these type of structures was founded in the literature [1]. Despite the large magnitude of this earthquake and the severe shaking records in Santiago, free-plan buildings showed good performance and remained essentially elastic with minor or no non-structural damage [2][3].

A variety of building models have been proposed to evaluate the seismic response of free-plan buildings, ranging from simpler models [4][5] to complex finite elements models (FEM) [6][7]. Recent technical reports provide guidelines on how to create structural models for tall buildings, e.g., PEER/ATC-72 [8] and LATBSDC [9] with a focus on Performance-Based Seismic Design (PBSD). Epistemic uncertainty represents the knowledge level in the modeling assumptions, and how it affects the predicted response. Free-plan buildings are particularly sensitive to epistemic uncertainty given their structural simplicity and low redundancy. To quantify this uncertainty at least three methodologies have been used: (i) stochastic FEM, where assumptions are variables that distribute with a probability density function [10]; (ii) sensitivity analysis, where some assumed variables



vary within discrete values [11]; and (iii) empirical measurements that reduce the uncertainty by calibrating model results with actual data [12].

Recent studies [4] as well as empirical evidence after the Maule earthquake have validated the importance of floor diaphragms in the flexural behavior of free-plan buildings. In common engineering practice, the diaphragm is modeled with infinite rigidity in-plane and infinite flexibility out-of-plane. This assumption enabled a reduction in the number of degrees of freedom (DOFs) of the model as well as in the required computational time. However, if the rigid diaphragm assumption is applied at levels with abrupt changes in lateral stiffness, such as the typical transition zone between the first level and first basement, a large shear stress is predicted within the core walls. This effect is known in the literature as *back-stay* effect [13]. Moreover, the consideration of the out-of-plane (bending) diaphragm stiffness becomes significant in the upper story shears [1][14].

Another important parameter in the dynamic response of free-plan buildings is the constraint imposed by the surrounding soil and the interaction thereof with the basement floors of the structure. Several approximations have been proposed for SSI models in high-rise buildings [15][16]. Most of these use simplified models by representing the soil through a discrete arrangement of springs and dampers to provide computational efficiency and reasonable accuracy. Additionally, seismic codes do not provide explicit recommendations on how to model the basements and the number of levels to include in the structural model to fix the model to the ground [17]. All these assumptions lead to discretionary interpretations that may lead to contradictory results in the design process. One example in the Chilean case is the definition of the level where to apply the minimum shear requirement in building design.

## 2. Selected buildings

Figure 1 show photographs of the six buildings selected for this study and referred to hereafter as Buildings A through F. All buildings have RC shear walls at the elevator core, a RC perimeter frame, and post tensioned RC slabs. The buildings are founded on firm soil (ASCE site class C [18]) and were all designed according to the Chilean code NCh433 [19] and ACI-318 [20]. Basic geometric data of the buildings are summarized in Table 1. The materials specified are H35 concrete ( $f'_c = 30$  MPa) and A630-420H reinforcement steel ( $f_y = 420$  MPa). Four of the investigated buildings (i.e. A, C, E and F) were in use at the time of the earthquake, and the other two buildings were near construction completion. None of the structures suffered any relevant structural, non-structural, or damage in contents [2][3]. Figure 2 shows, as a reference, 3D views, a typical floor plan, and an elevation of Building A.

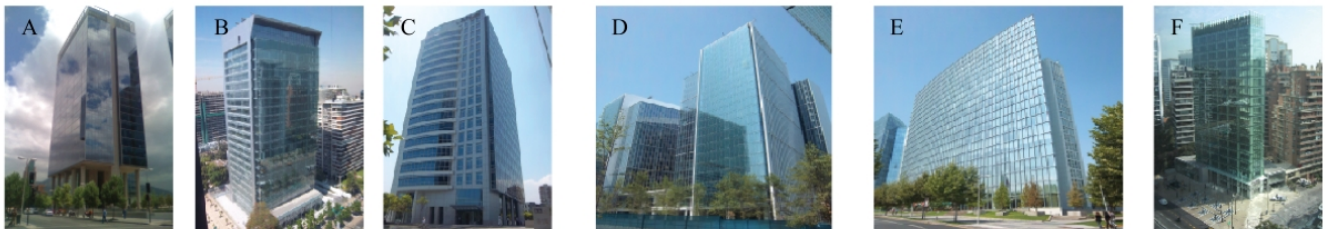


Fig. 1 – Overview of the buildings considered in the analysis

The selected buildings have between 19 and 24 stories and between 4 and 8 basements, and the total building height ( $H_t$ ) varies from 73 m to 105 m. The slenderness ratio ( $H_t / B$ ) varies between 2.4 and 5.0, and the typical floor area ( $A$ ) varies between 299 m<sup>2</sup> and 2,826 m<sup>2</sup> for the stories above ground. Analogously, the basement floor area ( $A_b$ ) varies between 1,023 m<sup>2</sup> and 7,361 m<sup>2</sup>. The thickness of RC floor slabs range from 16 cm to 28 cm, and considering the shear wall core area ( $A_c$ ) as the space used by elevators and staircases, the space efficiency ( $\eta_A = 1 - A_c / A$ ) in all buildings is over 84%. Core wall thicknesses ( $e_c$ ) range between 20 cm

in the top stories to 130 cm in the lower stories. The measured wall density with respect to floor area in each direction for a typical story ( $\rho_w^x$ ,  $\rho_w^y$ ) varies between 0.68% and 2.82%, but is usually less than 1.5%, i.e., about half the typical existing amount of residential shear wall buildings during the 1985 Chile earthquake, which was 2.8% average [21]. Additionally, fundamental periods were measured in all buildings with ambient vibrations [1], and led to first periods between 1.64s and 2.83s. The ratio of building height above ground level to first period ( $H/T_1$ ) is commonly used as a proxy of the global building stiffness, and varies between 29.7 m/s and 37.1 m/s, which based on a previous classification [22], indicated that these are flexible structures ( $H/T_1 < 40$  m/s).

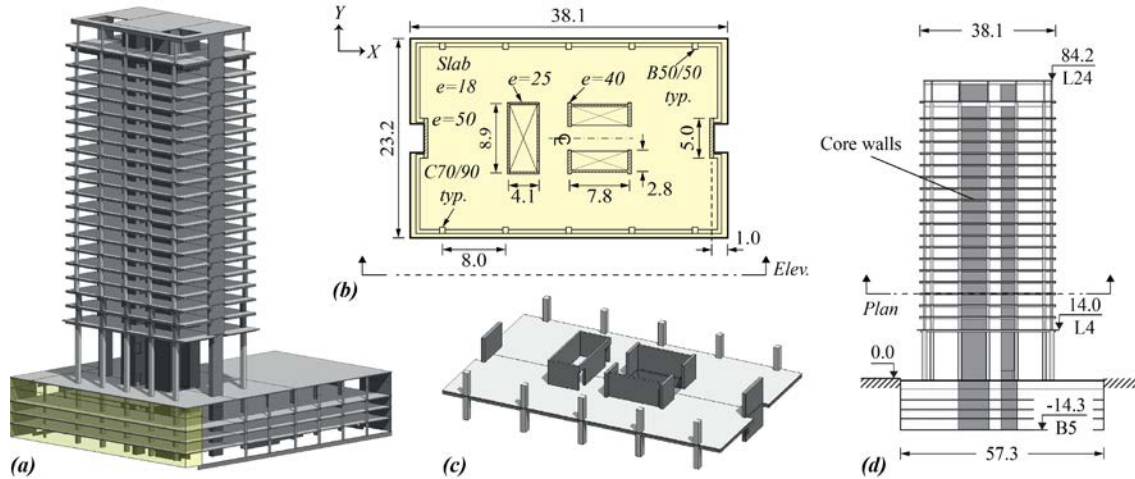


Fig. 2 – Schematic layout of typical Chilean free-plan buildings: (a) 3D view of render model; (b) typical floor plan; (c) typical 3D floor plan section; and (d) elevation. (dimensions are in meters and thicknesses of walls, slabs, and beams are in centimeters).

Table 1 – Geometric parameters of the studied buildings:  $N$  and  $N_b$  = number of stories above ground and below ground level, respectively;  $H$  = building height above ground level;  $H_t$  = total building height;  $A$  = typical floor area;  $A_b$  = typical basement floor area;  $\eta_A$  = space efficiency;  $\rho_w^x, \rho_w^y$  = shear wall density in X and Y direction, respectively;  $T_1$  = fundamental measurement period; and  $H/T_1$  = ratio of building height above ground level to first period.

Building	Number of stories $N + N_b$	Height (m)		Slender ratio $H_t/B$	Floor area (m <sup>2</sup> )		Space efficiency, $\eta_A$ (%)	Shear wall density (%)		Period (s) $T_1$	Ratio (m/s) $H/T_1$
		$H$	$H_t$		$A$	$A_b$		$\rho_w^x$	$\rho_w^y$		
A	24 + 5	84.2	98.5	4.2	874	3378	84	0.68	1.09	2.83	29.7
B	24 + 6	84.0	102.2	3.3	929	2963	84	1.56	2.82	2.26	37.1
C	23 + 7	81.7	105.2	3.2	1131	3932	85	0.71	0.80	2.51	32.6
D	22 + 8	74.9	99.6	2.4	2826	7361	86	0.99	1.19	2.42*	31.0
E	21 + 6	71.9	89.9	3.7	1553	5053	89	0.93	0.98	2.36	30.5
F	19 + 4	60.4	73.2	5.0	299	1023	89	2.03	1.52	1.64	36.9

\* measured period corresponding to right tower.

### 3. Estimation of the epistemic uncertainty

In order to estimate epistemic uncertainty in the structural models considered in this analysis (i.e. referred to as *variant* models), a *reference* model was defined by selecting common seismic design assumptions [8][9], i.e.: **(1)** slabs have finite in-plane and out-of-plane stiffness; **(2)** no consideration of SSI effects, i.e., model are fixed at the base; **(3)** basements are included in the model; **(4)** reinforced concrete is assumed to behave elastic, isotropic, and to remain uncracked; and **(5)** element gross sections neglect the contribution of the stiffness of the

reinforcement. For concrete, as FEM models are compared with ambient vibrations, a dynamic Young's modulus  $E_{dyn} = 1.2 E_c$  was assumed [23], where  $E_c$  is the static Young's modulus according to the ACI-318 [20] expression  $E_c = 4700\sqrt{f'_c}$  (MPa).

All six buildings were modeled in ETABS (ET) [24]. Also, two additional models were developed in ANSYS [25] using ANSYS *Parametric Design Language* mode (AP) for four buildings (A, C, D and F), and ANSYS *Workbench* mode (AW) for four buildings (A, B, E and F). Figure 3a shows as an example, the finite element model of Building A in its AP model version.

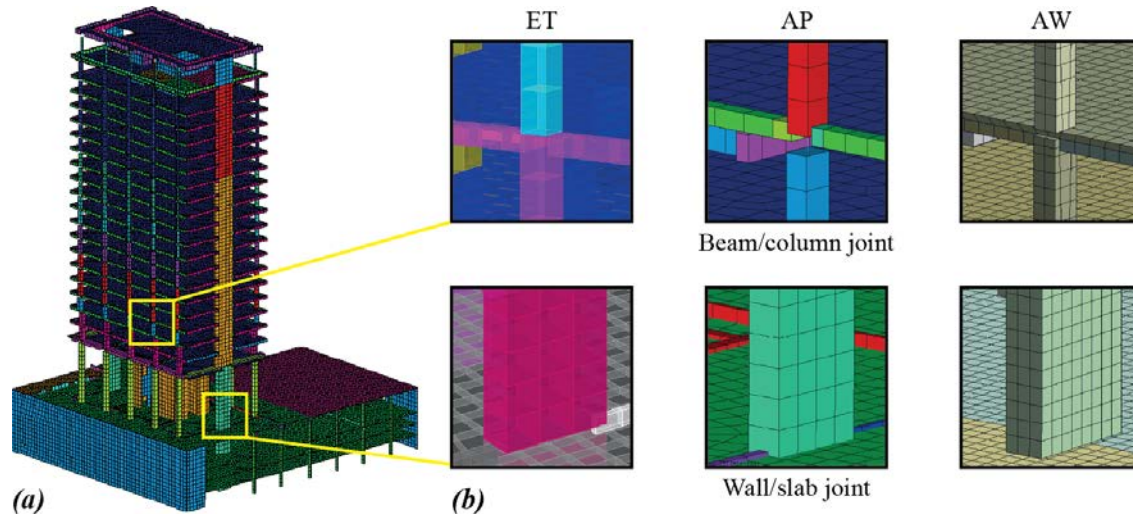


Fig. 3 – Schematic representation of the model: (a) Finite element model of Building A (AP model); and (b) type and connection among structural elements in beam/column joints and wall/slab joints in ET, AP, and AW models, respectively.

In addition to the modeling assumptions described previously, the considerations for each model are as follows: for ET and AP models, the beams and columns were modeled using 2-node Timoshenko frame type elements (ET: Beam and AP: BEAM44) with six DOFs per node, and rigid offset elements in beam-column joints (Figure 3b). The walls and slabs were modeled using shell type elements with six DOFs per node (ET: Shell with “thick-plate” stiffness and AP: SHEL181), where each use different formulations (ET: Mindlin-Reissner and AP: Dvorkin [26]). Additionally, in these models, all structural element connections considered mass overlap as well as a compatible mesh (Figure 3b), and for all beams embedded in a slab, the moment of inertia was multiplied by a factor to correct the bending stiffness provided by the slab.

For the AW models, all structural elements were modeled using 8-node brick elements (SOLID185) with three DOFs per node and an Enhanced Strain formulation [27]. In these models, incompatible meshes were generated independently for each structural element and were connected with contact elements (CONTA174 and TARGE170). Consequently, mass overlap was not generated in the connection of two elements. Finally, for the AP and AW models, masses in the elements were assigned to six DOFs per node and considered horizontal as well as vertical masses. ET models considered only the horizontal mass.

The number of nodes and elements in the ET models, with a maximum mesh size of 1.5 m, ranges between [17,690-90,912] and [19,330-103,895], respectively. Compared with the ET models, the AP models present 20% more nodes and 80% more elements, and the AW models between 9-14 times more nodes and between 10-17 times more elements. The total seismic weight ( $W_t$ ) of the ET models varies between 130.2 MN (Building F) and 1431.1 MN (Building D).

The seismic response of the buildings was estimated using modal response spectrum analysis using the elastic spectrum of the Chilean seismic isolation code, NCh2745 [28]. For the spectrum, a firm soil with a PGA



of  $0.41g$  was considered, with a maximum pseudo-spectral acceleration of  $1.2g$ , and 5% damping ratio. The seismic response is computed with at least 80% of the cumulative effective modal mass in each lateral direction ( $X$  and  $Y$ ). Thus, for the ET models, 100 modes were calculated using eigenvalues and eigenvectors, and for the AP and AW models, 250 modes were obtained using the Block Lanczos algorithm [29]. The input in both directions is independent, and the modal responses were computed by the Complete Quadratic Combination method (CQC).

The response parameters considered in this study are: **(1)** periods of the first four modes ( $T$ ); **(2)** story shear ( $V_i$ ) and shear carried by the core walls ( $V_c$ ), both expressed as a percentage of the total seismic weight ( $W_i$ ); **(3)** displacement of the geometric center of the diaphragm ( $u_c$ ) of each floor; and **(4)** lateral inter-story drift  $\delta_u = \Delta_u / h$ , where  $\Delta_u$  is the maximum inter-story displacement in each story in the direction of analysis, and  $h$  is the inter-story height.

The uncertainty of the response parameters for each modeling assumption is evaluated by analyzing the normalized ratio of the corresponding *variant* models ( $R_v$ ) and *reference* model ( $R_0$ ) results. These ratios are grouped by building as well as direction of analysis ( $X$  and  $Y$ ). Uncertainties in shear forces ( $V_i$  and  $V_c$ ) are evaluated at four levels: mid-height of the tower ( $H / 2$ ), base of the first story (L1), base of the first basement (B1), and base of the foundation level (BF). For all other responses, the uncertainty is evaluated only at levels where extreme values occur. The uncertainty of the ratios  $R_v / R_0$  is characterized by minimum and maximum values and standard deviation ( $\sigma$ ). Hereby graphical results are provided for the buildings that show the largest uncertainties to demonstrate the scatter of data due to the considered input assumptions.

Finally, the box-plots used hereafter have a rectangle whose length is the difference between the first and third quartile, a mean  $\bar{x}$  represented by an intermediate horizontal line, a median represented by a rhombus, whiskers equivalent in width to two standard deviations ( $2\sigma$ ), and outliers which fall outside the range ( $\bar{x} \pm \sigma$ ).

#### 4. Effect of diaphragm stiffness

The epistemic uncertainty due to the assumed diaphragm stiffness of the free-plan buildings is discussed here. The ET models were used to analyze four different diaphragm stiffness assumptions as shown in Figure 4a: **(i)** a semi-rigid diaphragm (DS), which considers in-plane and out-of-plane bending stiffness of the shell elements present in the slab at each floor (*reference* model); **(ii)** a semi-rigid diaphragm (DSo), which is identical to DS but with infinite flexibility out-of plane; **(iii)** a rigid in-plane diaphragm (DR), which considers an infinite in-plane stiffness but includes the out-of-plane stiffness of the shell elements at each floor; and **(iv)** a rigid in-plane diaphragm (DRo) but with infinite flexibility out-of-plane.

Figure 4b shows the first four periods of the DSo, DR and DRo models normalized with respect to the periods of the DS models (*reference* models) for the six buildings. Using the DS models as a reference, the first four periods of the DR models are up to 10% shorter. Contrarily, the first four periods of the DSo models are between 4% to 27% longer. Also, the first period of the DRo models are up to 19% longer. It is interesting to note that the different modeling assumption of the diaphragm can result in 37% difference in the first four periods. Moreover, the smallest differences are observed between  $T_{DR}$  and  $T_{DS}$ , which somewhat supports the historical assumption of using the DR model in practice instead of DS.

Figure 4c shows the vertical distribution of story shear  $V_i$  and core shear  $V_c$  in  $X$ -direction of Building B using the four diaphragm models. With respect to the effects of in-plane stiffness, estimated shears  $V_i$  and  $V_c$  in the DR and DRo models are consistently larger in all floors than those predicted by the DS and DSo models. This increase is more evident in the basements, where the base shear  $V_i$  predicted by the DRo model is 11.1%



larger than that predicted by the DSo model. Additionally, Figure 4c shows that the core shear  $V_c$  predicted by the DR and DRo models at level B1 are between 3.6 and 3.7 times larger than those predicted by the DS and DSo models, respectively. In fact,  $V_c$  is even 22% larger than  $V_t$  at level B1 for the DR and DRo models. This abrupt increase of shear forces in the core walls is attributed to the *back-stay* effect, as identified in the literature [13]. With respect to the bending stiffness, the predicted shears  $V_t$  and  $V_c$  of the DSo and DRo models are smaller than those predicted by the DS and DR models, respectively (at all floors). The largest difference is 27.9% for the core shear between the DS model and the DSo model. However, at the basements, the core wall  $V_c$  in DS-DSo models and the DR-DRo are similar.

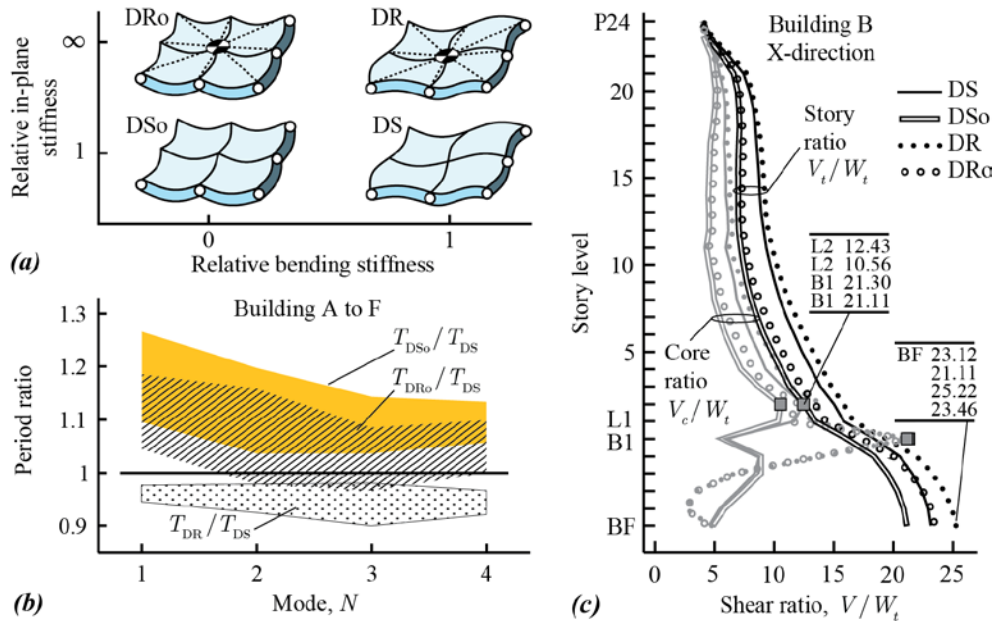


Fig. 4 – Epistemic uncertainty due to diaphragm stiffness: (a) models considered; (b) periods of the DSo, DR, DRo models normalized by those of the DS model for the six buildings, and (c) vertical distribution of story shear ratio  $V_t/W_t$  and core shear ratio  $V_c/W_t$  for Building B in the X-direction.

Figure 5 shows all normalized response parameters for the six buildings in the X- and Y-directions in box-plot format. The standard deviation ( $\sigma$ ) and the range between maximum and minimum of these ratios are shown in the accompanying table. Mainly due to the change in bending stiffness of the diaphragm, the normalized shears  $V_t$  and  $V_c$  above ground level ( $H/2$  and L1) vary between 0.75 and 1.44 with  $\sigma=13.3\%$ . Due to the change in the in-plane stiffness of the diaphragm, the normalized story shear  $V_t$  at the basements B1 and BF vary between 0.88 and 1.17 with  $\sigma=6.4\%$ . Additionally, due to the *back-stay* effect the normalized core shear  $V_c$  at the basements (B1 and BF), indicated in parenthesis in Figure 5, varies significantly between 0.57 and 4.29 with  $\sigma=112.2\%$ . From the values of the standard deviation, it is concluded that the uncertainty of the core wall shears  $V_c$ , is larger than that for the story shears  $V_t$ . Finally, the uncertainty of for the displacement  $u_c$  and inter-story drift  $\delta_u$  are smaller than those of story shear and core wall shear, and reach a maximum of  $\sigma=9.3\%$ .

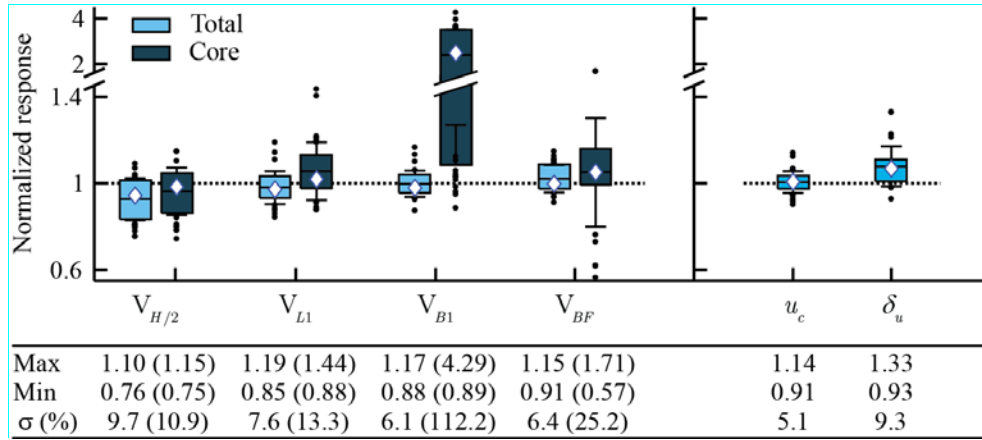


Fig. 5 – Response parameters of the DSo, DR and DRo models normalized by the results of the DS models for the six buildings: box-plot diagram (top); and maximum, minimum and standard deviation  $\sigma$  (%) (bottom). (Values in parenthesis associated with the core walls.)

### 5. Effect of the soil constraints

In order to study the epistemic uncertainty associated with the type of soil-structure interaction modeling assumptions, the AP models of four buildings (A, C, D and F), and the five modeling assumptions shown in Figure 6a were analyzed: **(i)** fixed support (SF) at the base of the structure (*reference* model); **(ii)** vertical springs support (SV) at the base of the structure; **(iii)** fixed support at the base but with lateral springs in the perimeter basement walls (SH) to account for the lateral stiffness provided by the soil; **(iv)** vertical and lateral springs support (SS)–combination of SV and SH; and **(v)** complete fixity (SB)–with all embedded elements fixed to the ground. In all models lateral displacements at the base level are assumed to be fixed.

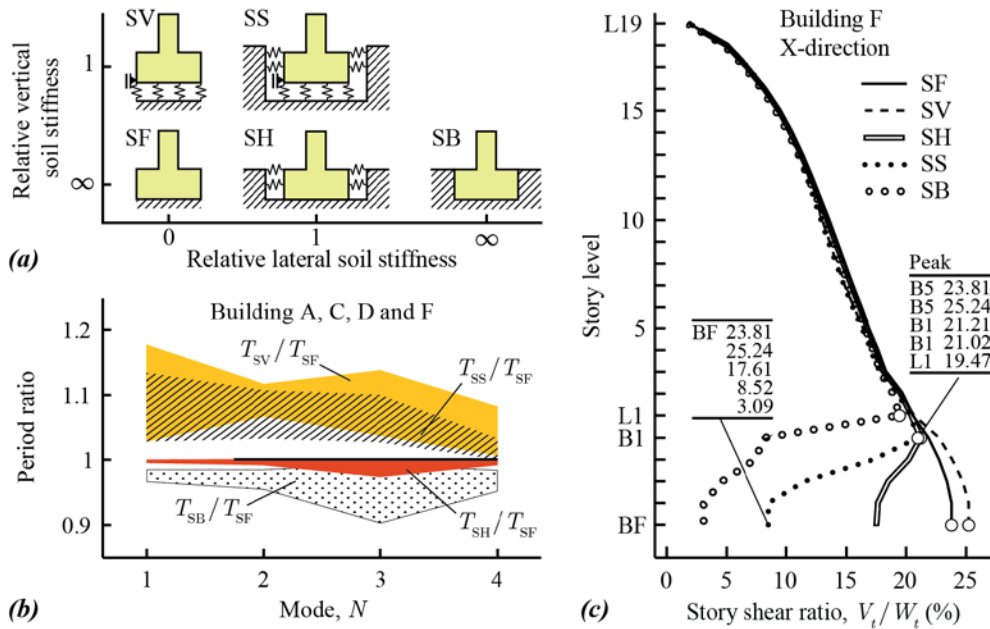


Fig. 6 – Epistemic uncertainty due to soil-structure interaction modeling assumptions: (a) models considered; (b) periods of the SV, SH, SS, SB models normalized by the SF model values for buildings A, C, D and F, and (c) vertical distribution of story shear ratio  $V_i / W_i$  for Building F in the X-direction.



To generate the SV, SH and SS models, a common soil profile was assumed for all buildings. The stratigraphy indicates very dense sandy gravel (class C per ASCE-7 [18]). The modulus of vertical subgrade reaction ( $K_v$ ) was considered constant for models with vertical springs, and the modulus of horizontal subgrade reaction ( $K_h(z)$ ) for this non-cohesive soil is proportional to the depth ( $z$ ). Due to stiff soil conditions, the inertial effects can be considered insignificant and the analysis is dominated only by the soil stiffness. The effect of the soil is represented with independent Winkler springs (COMBIN4). The stiffness of the springs used at the perimeter walls, slabs, and foundation beams, were proportional to the tributary area of each node of FEM model. For isolated column footings, rotational springs were added. More details of the soil parameters and spring stiffness values are documented in [1].

Figure 6b shows the first four periods of the SV, SH, SS and SB models normalized with respect to the SF values of buildings A, C, D and F. Using the SF models as a reference, the first four periods of the SV and SS models are up to 18% and 14% longer, respectively. Contrarily, the first four periods of the SH and SB models are between 3% and 10% shorter, respectively. Figure 6c shows the vertical distribution of story shear  $V_t$  predicted in the X-direction of Building F for the five modeling assumptions. In all cases, the story shears above ground level are very similar with a maximum difference of 3.4%. However, the SH, SS, and SB models predicts a reduced base shear  $V_t$ , with a minimum of 3.1% of the seismic weight predicted by the SB model i.e. 7.7 times less than that of the SF model. On the other hand, the SV model predicts a slight (6%) increase in the base shear  $V_t$  relative to the SF model.

Figure 7 shows all normalized response parameters for the four considered buildings in both directions ( $X$  and  $Y$ ) of analyses in box-plot format. The standard deviation ( $\sigma$ ) and the range between maximum and minimum of these ratios are shown in the accompanying table. Normalized story shears  $V_t$  and core shear  $V_c$  above ground level ( $H/2$  and  $L1$ ) vary between 0.80 and 1.10 with  $\sigma=6.1\%$ . Larger variability is predicted in the lower basements; where shears ratios vary between 0.24 and 1.64 with  $\sigma=27.3\%$  at level B1, and between 0.03 and 4.79 with  $\sigma=106.8\%$  at level BF. The presented results show that the standard deviation of the normalized core shear  $V_c$  is larger than that of the story shear  $V_t$  at all levels. The large variability of the shear forces at basements stems from the use of different soil elements and stiffnesses in the considered models, which in turn modifies the forces and reactions of the structure. Independently of this observation, the normalized parameters  $u_c$  and  $\delta_u$  show low variability with maximum  $\sigma=8.3\%$ .

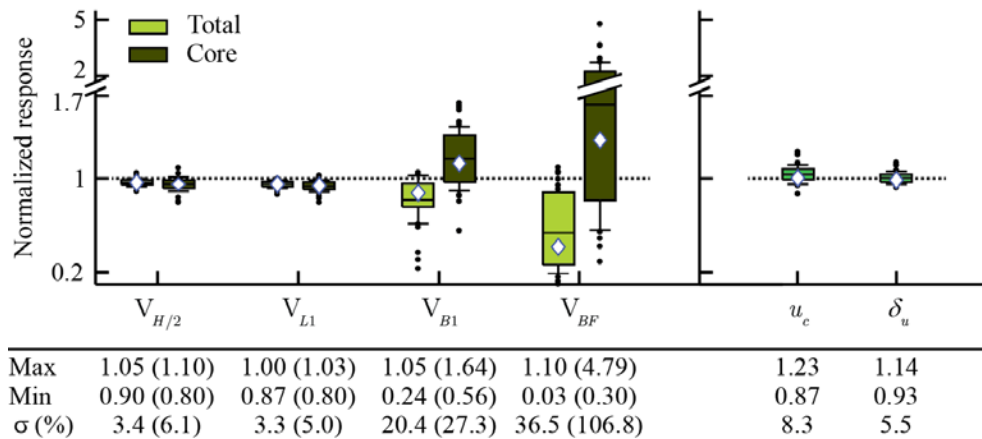


Fig. 7 – Responses parameters of the SV, SH, SS and SB models normalized by the results of the SF model for buildings A, C, D and F: box-plot diagram (top); and maximum, minimum and standard deviation  $\sigma$  (%) (bottom). (Values in parenthesis associated with the core walls.)

## 6. Uncertainty associated to assumed building fixity level

To investigate the uncertainty associated with “where” the building is assumed to be fixed, the AP and AW models for all buildings were used with different number of basements levels ranging from a model without basements to modeling all underground levels. A model with  $n$ -basements will be called  $U_n$  and is fixed to the ground at the bottom of  $n$ -th level at depth  $z_n$ . In this section  $U_0$  is the *reference* model, where the model is considered fixed at the bottom of first level. SSI effects have been omitted in this section.

Figure 8a shows the elongation of the first period ( $T_1^n / T_1^0$ ) for all buildings with the AP and AW models as a function of the normalized depth of the basement ( $z_n / H_b$ ). As expected, the period increases with the amount of basements considered, and the ratio  $T_1^n / T_1^0$  varies between 1.10 and 1.18 with  $\sigma=2.6\%$  when the normalized depth of 1.0 is considered (i.e. building fixed at the lower basement). Analogously, Figure 8b shows the story shear  $V_i$  at level L1 of model  $U_n$  ( $V_{i,L1}^n$ ) normalized with respect to  $U_0$  ( $V_{i,L1}^0$ ) expressed as a ratio  $r_1^n = V_{i,L1}^n / V_{i,L1}^0$ , for the four considered buildings and for the X- and Y-direction. A value  $r_1^n$  less than one implies that the story shear predicted at level L1 is reduced when the building model is fixed at  $n$ -th level. In other words, if the minimum code design shear is imposed at  $n$ -th level, the base shear at level L1 could be less than the minimum code design shear.

The story shear  $V_i$  at level L1 may in principle increase or decrease as the number of basements is added depending on the model and the direction of analysis. From figure 8b it is observed than the ratio  $r_1^n$  in buildings C and E in the X-direction reach a minimum of 0.84 and 0.96, respectively. Furthermore,  $r_1^n$  in buildings B and F in the Y-direction reach 1.2 and 1.1, respectively. In all cases, these peak values of the ratio  $r_1^n$  occur for  $z_n / H_b$  between 0.37 and 1.0.

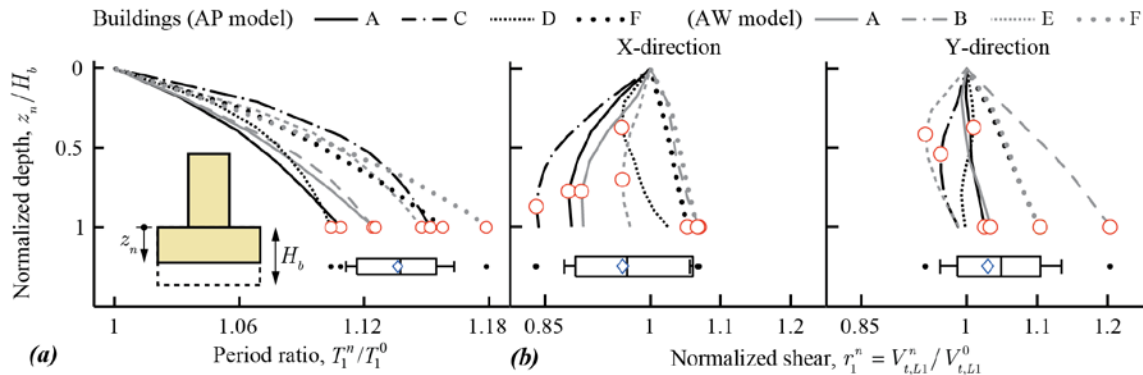


**Fig. 8** – Epistemic uncertainty due to the amount of basements considered in the models: (a) elongation of the first period  $T_1^n / T_1^0$  depending on the normalized depth of the basements ( $z_n / H_b$ ) for the six buildings; (b) normalized depth of basements ( $z_n / H_b$ ) versus normalized story shear at level L1 in all six buildings and the X- and Y-directions, respectively.

Figure 9 shows all normalized response parameters for the buildings considering different building fixity level and for both directions of analysis (X and Y), in box-plot format. As before, normalization is performed by dividing all  $U_n$  responses by the *reference*  $U_0$  response. The standard deviation ( $\sigma$ ) and the range between maximum and minimum of these ratios are shown in the accompanying table. The variability of the normalized story shear  $V_i$  and core shear  $V_c$  ranges at level L1 between 0.67 and 1.23 with  $\sigma=10.5\%$ . In terms of standard deviation and range, the uncertainty of the normalized core shear  $V_c$  at levels  $H/2$  and L1, shown in parenthesis, is larger than that the normalized total shear  $V_i$ . Analogously, the normalized displacement  $u_c$

varies between 1.00 and 1.36 with  $\sigma= 10.8\%$ , and the normalized drift  $\delta_u$  has  $\sigma= 6\%$ . The standard deviation of all normalized responses is less than 11%.

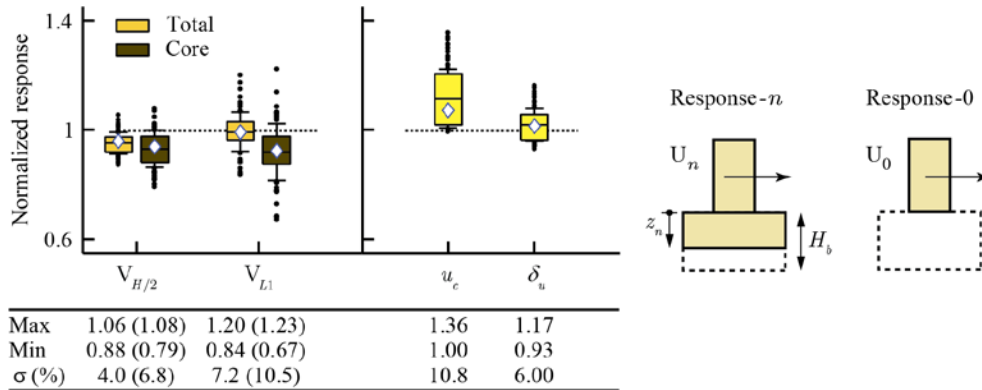


**Fig. 9** – Response parameters of the  $U_n$  models normalized with respect to the  $U_0$  models for the six buildings considered in this analysis: box-plot diagram (top); and maximum, minimum and standard deviation  $\sigma$  (%) (bottom). (Values in parenthesis associated with the core walls.)

## 7. Summary and Conclusions

This study evaluates epistemic uncertainty in building models intended to compute response parameters such as periods, story shears, and inter-story drifts. Inherent uncertainty occurs due to three important structural modeling assumptions: **(1)** the diaphragm stiffness; **(2)** the soil-structure interaction model; and **(3)** the amount of basement levels considered. Several finite element models (FEM) models were used to analyze six reinforced concrete buildings located in Santiago, Chile. Then, numerical FEM models were used to study sources of epistemic uncertainty in terms of standard deviations ( $\sigma$ ) of the normalized response parameters, where several *variant* models were compared with *reference* models, defined with common design assumptions. This study has led to the following conclusions:

- The diaphragm stiffness was found to be one of the most important sources of epistemic uncertainty. Diaphragm stiffness variations modified the first four building periods by either shortening (-10%) or elongating (+27%) the building periods when compared with a *reference* model that includes the in-plane and bending stiffness of the slab. Normalized story shear  $V_t$  and core shear  $V_c$  at building mid-height ( $H/2$ ) are influenced mainly by variations in the bending diaphragm stiffness, and vary between 0.75 and 1.44 with  $\sigma= 13.3\%$ . Contrary, at basements, in-plane stiffness variation are important and causes the normalized total shear  $V_t$  to vary between 0.88 and 1.15 with  $\sigma= 6.4\%$ . The largest variation of normalized shear  $V_c$  occurs at the first basement level, with a range of [0.57-4.29] and  $\sigma= 112.2\%$ , and is attributed to the *back-stay* effect.
- Regarding the epistemic uncertainty related to the type of Soil-Structure Interaction (SSI) model used, variations in the first four building periods range from -10% to +18% when compared with a *reference* model with a fixed base. The distribution of normalized shears  $V_t$  and  $V_c$  above ground level were found to be similar, however, shear force distribution at the basement levels strongly depend on the soil-structure interaction model used. Normalized shears  $V_t$  and  $V_c$  at the first basement level vary between 0.24 and 1.64 with  $\sigma= 27.3\%$ , and at the base level between 0.03 and 4.79 with  $\sigma= 106.8\%$ .
- The uncertainty associated with the fixity level of the model to the ground showed a first period variation ranging from +10% to +18% relative to the *reference* model without basements. The total story shear  $V_t$  at the first story either increases or decrease as more basements are added into the structural model. Base shear



values range between 0.84 and 1.2 with respect to the *reference* model and depending the level at which the minimum base shear is imposed into the model, results may lead to conservative or unconservative designs. In all cases studied, peak values occur as fixity is imposed at intermediate underground levels. Variations in all responses yielded  $\sigma$  less than 10.8%.

- Finally, it is concluded that from all sources of epistemic uncertainty characterized in terms of standard deviations of the normalized responses, larger uncertainty can be identified in free-plan buildings associated with the core shear  $V_c$  rather than the total story shear  $V_t$ . Additionally, the uncertainty is larger in shears  $V_t$  and  $V_c$  at basements (B1 and BF) than in the upper levels ( $H/2$  and L1).

## Acknowledgements

This research has been funded by Grants CONICYT/Fondecyt/1141187, CONICYT/FONDAP/15110017 (National Research Center for the Integrated Management of Natural Disasters, CIGIDEN), and CONICYT/Doctorado Nacional/2013. The authors are very grateful for the support provided by the researchers Anne Lemnitzer, Rosita Jünemann and Joao Marques.

## References

- [1] Chacón MF, de la Llera JC, Hube MA, Marques J, Lemnitzer A (2016): Epistemic uncertainty in the seismic response of RC free-plan buildings, Submitted to *Engineering Structures*.
- [2] Naeim F, Lew M, Carpenter L, Youssef N, Rojas F, Saragoni G, Schachter M (2011): Performance of tall buildings in Santiago, Chile during the 27 february 2010 offshore Maule, Chile earthquake, *The Structural Design of Tall and Special Buildings*, **20** (1) 1–16.
- [3] Lemnitzer A, Massone LM, Skolnik DA, de la Llera JC, Wallace JW (2014): Aftershock response of rc buildings in Santiago, Chile, succeeding the magnitude 8.8 Maule earthquake, *Engineering Structures*, **76**, 324–338.
- [4] Encina J, de la Llera JC (2013): A simplified model for the analysis of free plan buildings using a wide-column model, *Engineering Structures*, **56**, 738–748.
- [5] C. Sepúlveda, J. C. de la Llera, A. Jacobsen (2012): An empirical model for preliminary seismic response estimation of free-plan nominally symmetric buildings using ANFIS, *Engineering Structures*, **37**, 36–49.
- [6] Shin M, Kang THK, Grossman JS (2010): Practical modelling of high-rise dual systems with reinforced concrete slab-column frames, *The Structural Design of Tall and Special Buildings*, **19** (7), 728–749.
- [7] Lu X, Lu X, Zhang W, Ye L (2011): Collapse simulation of a super high-rise building subjected to extremely strong earthquakes, *Science China Technological Sciences*, **54** (10), 2549–2560.
- [8] ATC-72 (2010), Modeling and acceptance criteria for seismic design and analysis of tall buildings, *Applied Technology Council (ATC) and Pacific Earthquake Engineering Research Center (PEER)*.
- [9] LATBSDC (2014): An alternative procedure for seismic analysis and design of tall buildings located in the Los Angeles region, *Los Angeles Tall Buildings Structural Design Council (LATBSDC)*.
- [10] Hardyniec A, Charney FA (2012): The effect of epistemic uncertainties in the assessment of seismic collapse of building structures, *10<sup>th</sup> U.S. National Conference on Earthquake Engineering*, Anchorage, Alaska.
- [11] Sousa R, Eroğlu T, Kazantzidou D, Kohrangi M, Sousa L, Nascimbene R, Pinho R (2012): Effects of different modelling assumptions on the seismic response of rc structures, *15<sup>th</sup> World Conference of Earthquake Engineering*, Lisboa, Portugal.
- [12] Brownjohn J, Pan T, Deng X (2000): Correlating dynamic characteristics from field measurements and numerical analysis of a high-rise building, *Earthquake Engineering & Structural Dynamics*, **29** (4), 523–543.
- [13] Rad BR, Adebar P (2009): Seismic design of high-rise concrete walls: Reverse shear due to diaphragms below flexural hinge, *Journal of Structural Engineering*, **135** (8), 916–924.



- [14] Lee DG, Kim HS, Chun MH (2002): Efficient seismic analysis of high-rise building structures with the effects of floor slabs, *Engineering Structures*, **24** (5), 613–623.
- [15] Naeim F, Tileylioglu S, Alimoradi A, Stewart JP (2010): The Real Deal on Soil-Foundation-Structure Interaction (SFSI), SEAOC Convention Proceedings.
- [16] Li M, Lu X, Lu X, Ye L (2014): Influence of soil–structure interaction on seismic collapse resistance of super-tall buildings, *Journal of Rock Mechanics and Geotechnical Engineering*, **6** (5), 477–485.
- [17] Kim S (2001): Efficient seismic analysis of high-rise buildings considering the basements, *New Zealand Society for Earthquake Engineering*, Conference, n° 4.
- [18] ASCE/SEI-7-10, Minimum Design Loads for Buildings and Others Structures, American Society of Civil Engineers.
- [19] NCh433, Earthquake Resistant Design of Buildings (in Spanish), *Instituto Nacional de Normalización* (INN), Santiago, Chile.
- [20] ACI-318, Building code requirements for structural concrete and commentary (318-05), *American Concrete Institute* (ACI), Detroit, Michigan.
- [21] Jünemann R, de la Llera JC, Hube M, Cifuentes L, Kausel E (2015): A statistical analysis of reinforced concrete wall buildings damaged during the 2010, Chile earthquake, *Engineering Structures* **82**, 168–185.
- [22] Guendelman M, Lindenberg J (1996): Perfil bio-sísmico de edificios, *VII Jornadas Chilenas de Sismología e Ingeniería Antisísmica*, ACHISINA, La Serena.
- [23] Lydon F, Balendran R (1986): Some observations on elastic properties of plain concrete, *Cement and Concrete Research*, **16** (3), 314–324.
- [24] ETABS, Integrated Building Design Software ETABS Nonlinear version 9.7.4, Reference Manual, *Computer and Structures, Inc.* (CSI), Walnut Creek, California.
- [25] ANSYS, ANSYS® Academic Research, Release 12.1, *ANSYS, Inc.*, Canonsburg, Pennsylvania.
- [26] Bathe KJ, Dvorkin EN (1986): A formulation of general shell elements? the use of mixed interpolation of tensorial components, *International Journal for Numerical Methods in Engineering* **22** (3) (1986) 697–722.
- [27] Simo JC, Armero F, Taylor R (1993): Improved versions of assumed enhanced strain tri-linear elements for 3D finite deformation problems, *Computer Methods in Applied Mechanics and Engineering*, **110** (3), 359–386.
- [28] NCh2745, Earthquake-Resistant Design of Base-Isolated Buildings (in Spanish), *Instituto Nacional de Normalización* (INN), Santiago, Chile.
- [29] Grimes RG, Lewis JG, Simon HD (1994): A shifted block Lanczos algorithm for solving sparse symmetric generalized eigenproblems, *SIAM Journal on Matrix Analysis and Applications*, **15** (1), 228–272.